Brazilian Journal of Geophysics 42 (2024), 2, 1-29
Brazilian Geophysical Society
ISSN 2764-8044
DOI: 10.22564/brjg.v42i2.2310

IMPACT OF 4D SEISMIC DATA ASSIMILATION IN THE PRODUCTION FORECASTING OF A HEAVY OIL TURBIDITE SANDSTONE FIELD OFFSHORE BRAZIL

Felipe Bruno Mesquita da Silva, Alessandra Davolio, and Denis José Schiozer

Universidade de Campinas - Unicamp, Campinas - SP, Brazil

*Corresponding author email: fmesq@unicamp.br

ABSTRACT. The incorporation of 4D seismic data can be done at model characterization and data assimilation steps, the latter applying the observed data to update the model properties. In this work, we evaluate the impact of 4DS data in the production forecasting results investigating the influence on these distinct steps. We employ a prior model set generated without 4DS data and another prior set with 4DS in the characterisation. We perform, then, the DA in three different ways: (1) using only well history data with a prior set without 4DS; (2) using well history and 4DS data with this same prior set; and (3) using well history and 4DS data with the prior set generated with 4DS data. We employ the Ensemble Smoother with Multiple Data Assimilation method for data assimilation and implement a procedure to adjust the well productivities and injectivities after DA. This work assesses the differences among the three DA cases in terms of field oil production forecasting, model attributes and model misfits, the latter evaluated in terms of the assimilated data set and of a different data set for validation purposes only. We apply the work to a real heavy oil turbiditic field located offshore Brazil. The case application demonstrates a successful data assimilation study on a real field integrating well history and 4DS data. The results show that the utilisation of 4DS in both model characterisation and DA steps brought value to the final uncertainty reduction results. The posterior model ensemble with 4DS data in model characterization and DA provided the lowest model misfits overall to the full data set, being the best choice for application in field production forecasting studies. The case without 4DS data provided significantly more pessimistic field oil production than the cases with 4DS, making very evident the importance of employing 4DS at uncertainty reduction workflows.

Keywords: Permanent Reservoir Monitoring; reservoir simulation; data assimilation; uncertainty reduction; heavy oil field

INTRODUCTION

The decision-making process in development and management activities of oil and gas fields has to deal with uncertainties related to the representation of the reservoir (uncertain rock, fluid and rock-fluid properties), which can be highly uncertain due to the impossibility of measuring properties at each spatial point of the reservoir volume. For this reason, simulation models are an important tool since it

can integrate all available information obtained from the reservoir, and represent it as model uncertainties. The final goal is to perform the most reliable as possible field production forecasting to take more assertive decisions. After a decision is made and applied in the field, the dynamic data in response to the change in field operation is measured and assimilated in the model updating process to support further decisions, framework named as closed-loop. There are several closed-loop methodologies published in the literature to handle the development and management of field production. Paiaman et al. (2021) present a review of such methods, being Brouwer et al. (2004) the first publication on life-cycle closed-loop practice.

Schiozer et al. (2019) propose a general methodology to guide the closed-loop field development and management (CLFDM) dividing the process at steps, grouped in four main parts identified by colours in Figure 1. This methodology allows performing reservoir simulation studies under a well-structured framework that facilitates the conduction of tasks and decisions, making the decision process less subjective. This work is mainly related to the red part (uncertainty reduction), with link to the green part (model characterisation and construction).

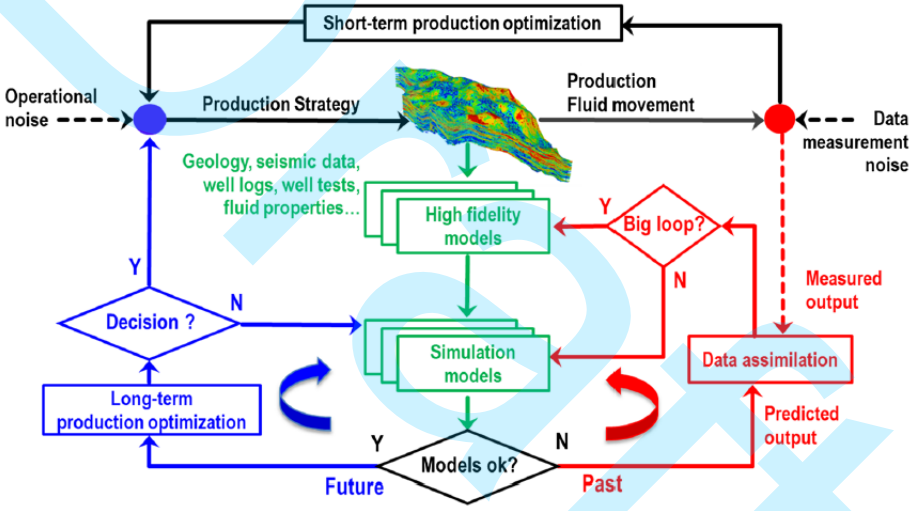

Figure 1: Closed-loop reservoir development field development and management (CLFDM) workflow (Schiozer et al., 2019).

The green part comprises the reservoir characterisation and modelling process. It initiates by gathering all available data about the field, such as general geological information (e.g. analogue outcrops, stratigraphic chart), seismic data, well logs, well testing, PLT (production logging tool), and petrophysical laboratory measurements. All this information is then used to build a detailed geological model. The final product of the model characterisation and modelling process is a prior ensemble of simulation models, normally after upscaling of the geological model, which will be employed in the red part of the workflow in Figure 1.

The red part consists of the data assimilation (DA) process, a probabilistic process that assimilates, using the prior simulation model ensemble as input, the dynamic observed data at the field. The global objective is to reduce the variance of the uncertain reservoir properties while improving the model fit to

the dynamic data. The output of the red part is an ensemble of models (posterior simulation model ensemble) that ideally honour all the observed data according to a tolerance. This posterior model ensemble is applied, then, in decision analysis (blue part in Figure 1).

One key dynamic data that has become progressively more available is the 4D seismic (4DS) or time-lapse seismic data. It can provide important information on the fluid dynamics at inter-well locations or even stratigraphy (Maleki et al. 2017). There are mainly three different domains in which 4DS data can be applied in DA: (1) seismic amplitudes, (2) calculated pressure or saturation changes and (3) inverted impedances. In the first, we compare the acquired amplitude differences to the synthetically derived results of simulation models from forward modelling, which can be computationally expensive. Some studies use this type of data for 4DS data assimilation, such as van Gestel et al. (2011), Yin et al. (2019) and Soares et al. (2020). In the second domain, we invert seismic data to estimate pressure and saturation changes, which are directly used as input to improve the model fit (De Souza et al., 2010), but this process is highly uncertain. In Fahimuddin et al. (2010), the authors conclude that the third domain (4DS impedance data) provides better well performance and seismic model fits in relation to 4DS amplitudes. Some examples of application of this type of domain can be found in Emerick and Reynolds (2013a), Lorentzen et al. (2020), Neto et al. (2021), and Silva Neto et al. (2021). Acoustic impedances are obtained by the inversion of seismic amplitudes, being the most common data used in DA studies nowadays (Oliver et al., 2021) and have been chosen as the domain to apply 4DS data in data assimilation.

There are several manners of utilising 4DS data in conjunction with well history data in dynamic models. The work of Rosa et al. (2022) introduced some of them, being the iterative ensemble smoother (ES) a successful method to assimilate large amounts of seismic and well history data (Fossum and Lorentzen, 2019). The ensemble smoother with multiple data assimilation (ES-MDA), proposed by Emerick and Reynolds (2013b), is an extension of the ES method, which circumvents the issue of time-consuming simulation restarts that occur at the sequential data assimilation originally introduced by Evensen (1994). ES-MDA is currently the state-of-the-art method in data assimilation according to Maschio et al. (2022), and it has been chosen as the method to perform the DA.

Oliver et al. (2021) presents a history of 4DS application at data assimilation (DA) or, as named by the author, 4DS history matching. There exist numerous applications of ES-MDA in 4D seismic history matching. Some of them can be mentioned, such as Emerick and Reynolds (2013a), Leeuwenburgh and Arts (2014), da Nobrega et al. (2018), and Yin et al. (2019).

According to Oliver et al. (2021), while methodologies for DA of 4DS data have demonstrated substantial value in synthetic model studies, the application to real fields has not been as successful. The effects of model error appear to be more pronounced in DA of 4DS data than in traditional DA of well history data due to the following reasons: additional need for modelling the seismic attributes from reservoir simulation models, and the demanded work to handle the data volume including the definition of a reliable petro-elastic model (PEM) and of an appropriate seismic attribute to be employed. Yet, applications to field cases appear to have been at least partially successful, although quantitative

assessment of the model misfits and the improvements in forecast is difficult (Oliver et al., 2021).

Several authors employed the case studied in this work, named S-Field, at different steps of 4DS data analysis and uncertainty reduction. Maleki et al. (2021) introduce a stepwise workflow to reduce the uncertainties in the 4DS interpretation and to identify the improvements required for better reservoir surveillance. Maleki et al. (2022) illustrate the importance of employing multiple 4DS datasets for improved field management. Correia et al. (2023) extend a previously proposed workflow that generates prior simulation models with geological consistency to incorporate the 4DS data interpreted from Maleki et al. (2022) in the model characterisation and calibrate it through a forward geomodelling approach. Maschio et al. (2022) propose a methodology to generate and evaluate the performance of lower-fidelity models (LFM) combined with the application of ES-MDA method assimilating well history data. The authors employ a prior set of models generated before the work of Correia et al. (2023). Santos et al. (2022) present a workflow to quickly quantify the errors between simulation model ensembles and observed 4DS data by similarity indicators. Rosa et al. (2022) discuss the impact of using the original simulation grid (more refined) versus the most efficient LFM grid (coarser) from Maschio et al. (2022), and the effect of using different 4DS data resolutions in the results of DA and production forecasting. Among other conclusions, Rosa et al. (2022) state that the original grid is more sensitive to the different 4D seismic inputs and yields estimates of acoustic impedance changes visually closer to the observed data than those obtained from the coarser grid. The other important conclusion from these authors in the context of the present work is the application of further 4DS information at two maps instead of a single map, which is able to predict important reservoir behaviours such as the gas trapping in the deepest interval.

This work evaluates the impact of applying 4DS data in model characterisation and data assimilation steps to the field production forecast. Similar to Rosa et al. (2022), it utilises the original simulation grid and the 4DS information at two maps in the DA process, with the same settings of petro-elastic modelling as it was done by Santos et al. (2022) and the previous authors. Different from Rosa et al. (2022), this work employs prior simulation model ensembles that are better calibrated to well history data than in the previous S-Field works, and separate prior sets incorporating or not the 4DS information in the model characterisation. Additionally, this work introduces procedures to help deciding which posterior model ensemble is better in relation to the field dynamic data (well history and 4DS data), what may be an important contribution to real field applications. The main novelty of the present work lies in the evaluation of 4D seismic data application at model characterization step in a data assimilation framework comparing the use of 4DS data with the (traditional) use of just well history data.

Objective

The objective of this work is to evaluate the impact to field production forecasting results of applying 4D seismic data in the uncertainty reduction workflow that traditionally utilises only well history data as dynamic information. We investigate, in a systematic manner, the use of 4DS in the model characterisation and data assimilation steps, and confront these results with the case in which only well

history data is used.

METHODOLOGY

Figure 2 shows a general scheme of the proposed methodology. It is developed in the context of the CLFDM workflow published by Schiozer et al. (2019), focused at the uncertainty reduction step (red part of Figure 1).

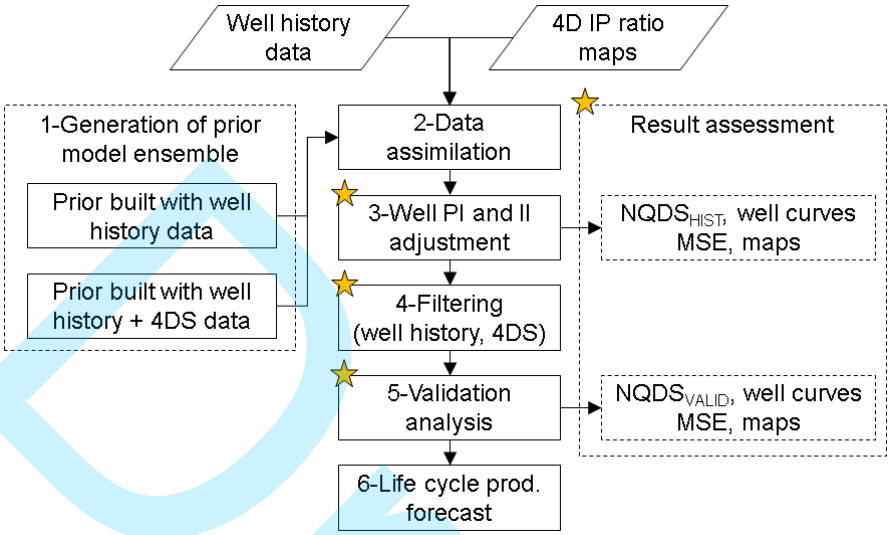

Figure 2: General scheme of the proposed methodology, with the contributions highlighted with a yellow star.

The main steps of the developed methodology are: (1) generation of prior model ensembles being one built with well history data and another one built with well history data + 4DS data, (2) data assimilation of dynamic data (4DS, well history data), (3) well productivity index (PI) and injectivity index (II) adjustment, (4) filtering with all available dynamic data, (5) validation analysis and (6) life-cycle production forecast.

At the first step, we generate the different prior model ensembles to evaluate the influence from the 4DS data incorporation at the model characterisation step. In the data assimilation (DA) step, we assimilate the dynamic data whose impact will be evaluated in the study. It is important to mention that we assimilate a very different number of data points when we assimilate or not the 4DS data, since this data set contains spatial information, which is not present at the well history data set. As a consequence, the assimilation of 4DS data is expected to lead to more uncertainty reduction (more reduction in the variability of model properties).

The step 3, well PI and II adjustment, consists of adjusting the productivity and injectivity of the wells by using the end of the well history data period available in order to improve the simulation model results in the transition from past (history) to future (forecast) conditions. This is important to allow a proper comparison between the simulation model results and the well production and injection measured data during a time period that has not been employed at the uncertainty reduction process. This comparison is named as validation in this work (step 5 in the proposed methodology, Figure 2) and is intended to

evaluate the capacity of the posterior model ensemble to reproduce the measured data in the field.

After the adjustment of well PI and II, we perform the filtering step with all available dynamic data (well history, 4DS data), and the models that can pass simultaneously the acceptance criteria of all dynamic data proceed to the validation analysis. This validation is made in an attempt to increase the confidence in applying the posterior model ensemble in the life-cycle production forecasting (step 6 of the methodology), and make more assertive decisions on field development and management activities.

We assess the results in qualitative and quantitative means after the well PI and II adjustment by employing all the data that has been assimilated (4DS, well history data). Finally, we perform the validation analysis by confronting the simulation model results with all the measured data that has not being applied previously (blind test), and run the life-cycle production forecast.

Well PI and II Adjustment

After the data assimilation, we develop and apply a procedure to adjust the well productivities and injectivities. This is made because of the difficulties faced, with the ES-MDA method, to obtain satisfactory results from the simultaneous assimilation of well data time series and the PD (productivity deviation) function that was proposed in Almeida et al. (2018), Formentin et al. (2019).

Similar to the previous works, we simulate the posterior model ensembles by switching the informed data series from well rate (Ql for producers and Q_{wi} for injectors) to BHP at the last simulation time of well operation. Differently from the previous works, we adjust the well productivity and injectivity indexes (PI and II) after DA of the well data time series, according to Equations 1 and 2, respectively.

$$PI_{modified} = PI_{previous} \times \frac{Q_{l,HIST}}{Q_{l,model}} \qquad (1)$$

$$II_{modified} = II_{previous} \times \frac{Q_{wi,HIST}}{Q_{wi,model}} \qquad (2)$$

$PI_{previous}$ and $II_{previous}$ are the indexes obtained after the DA previously completed. $Q_{l,model}$ and $Q_{wi,model}$ are the respective liquid production and water injection rate at the last simulation time of well operation, date when the informed data is switched from well rate to BHP. $Q_{l,HIST}$ and $Q_{wi,HIST}$ are the respective well rates from the history data on this date. As a consequence of the Equations 1 and 2, if the simulated model well rate equals the history data, the well productivity or injectivity does not need any adjustment, and the respective PI or II value will not be modified. The application of Equations 1 and 2 assumes that there is not a significant misfit between the simulated and the history BHP data at the last simulation time of well operation (BHP employed as informed data to the simulator).

Validation Analysis

After the adjustment of productivity and injectivity index of the wells, we extend the simulation time period from the end of the history period until the end of the measured data by keeping the BHP of the wells as informed data to the simulator. The well shutdown dates occurred in the field must be informed in the simulation model.

We perform the comparative analysis between the simulation model results and the measured data by employing the same time frequency of data that has been assimilated at the step 2 of the methodology. For example, if daily well rates were assimilated, then we employ daily well fluid rates in the validation analysis (not cumulative fluid volumes). This is recommended to be more rigorous in terms of the predictive capacity of the simulation models.

APPLICATION

Field Description and Data Available

The case study is a real field of heavy oil (16º API), a turbiditic sandstone reservoir that is structurally and stratigraphically trapped located offshore Campos Basin, Brazil, named as S-Field. The field oil production started on October 1st, 2013 and the water injection, 143 days later. The time period of available well production and injection data, and seismic acquisitions is 2359 days (6.5 years).

The well production and injection data include, on daily basis: oil production rate (Q_o), water production rate (Q_w), gas production rate (Q_g) and average bottom-hole pressure (BHP) from eight oil production wells, and water injection rate (Q_{wi}) and BHP from four water injectors. The wells follow, predominantly, a nearly horizontal trajectory in the reservoir. Figure 3 presents a grid top map view of base layer of the main sand with all well completions shown. The seismic data comprise three PRM (permanent reservoir monitoring) seismic acquisitions, being one base survey acquired 60 days after field production start-up and two monitors: m3 (911 days) and m5 (2299 days).

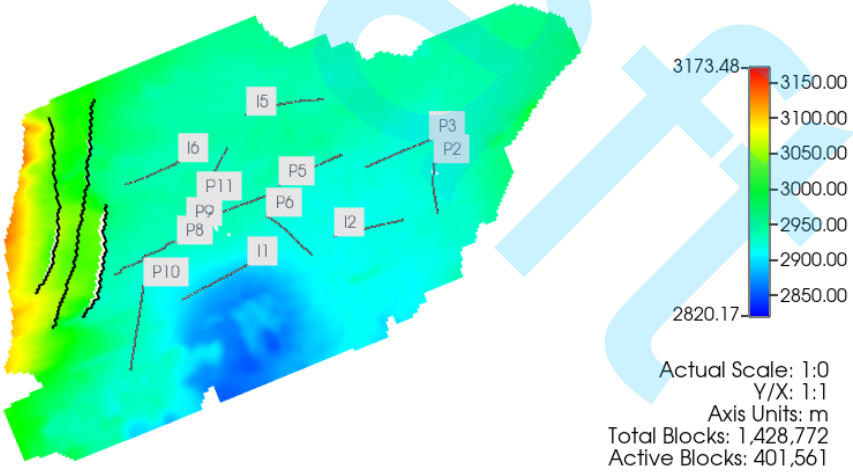

Figure 3: Top map view of main sand base of S-Field simulation model (K-48) including all the well locations. Wells starting with “P” are oil producers and those with “I”, water injectors.

We consider the history period from day 1 to 2298 (6.3 years), and validation period - in order to evaluate the predictive capacity of the models in relation to the measured data in the field - from day 2299 to 2359 (2 months).

Simulation Model

The simulation grid is of corner-point type and the reservoir fluid is treated by a black-oil model. The bottom aquifer is modelled numerically and the aquifer body in the lateral vicinity of the reservoir grid is modelled analytically by Fetkovitch method. Table 1 presents the grid size for each reservoir interval. These intervals follow the same definitions of Rosa et al. (2022) in order to apply their two maps of observed 4DS data in the main sand of the reservoir.

Table 1: Simulation grid size by reservoir interval.

Reservoir interval	Number of grid cells			Average block size (m)			Active grid cells
	N_I	N_J	N_K	I	J	K	
Top-middle of main sand	218	113	38	50	50	1.5	174,460
Middle-base of main sand	218	113	10	50	50	1.5	174,876
Extra sand	218	113	10	50	50	8.0	54,392

This work uses the liquid production rate (QI) as boundary condition informed to the simulator for the production wells and water injection rate (Q_{wi}) for the injectors at the data assimilation step (history period), and BHP at the last simulation time of well operation (last date of history) and during the validation period.

Generation of Prior Model Ensembles with and without 4DS

An ensemble of 200 equiprobable petrophysical image realisations of porosity, net-to-gross (NTG), horizontal absolute permeability and rock type, totalling 800 images with approximately 400,000 active grid blocks each, is generated in the model characterisation step of CLFDM workflow (Schiozer et al., 2019).

The sequential indicator simulation is employed to generate the rock type realisations. The sequential gaussian simulation technique generates the porosity, NTG and horizontal absolute permeability. The 3D impedance from base survey is utilized as a secondary variable for the generation of porosity. The uncertain variables used in the generation of the image realisations include the variogram range for rock type, porosity, horizontal absolute permeability and NTG, and the correlation coefficients between porosity and permeability (log-normal distribution), impedance and porosity (normal distribution), and NTG and porosity (normal distribution). After the generation of the image realisations, the images are calibrated with well history data. This model ensemble is employed and named in this work as Prior_no4DS, which is the prior simulation model ensemble with no application of 4DS data in the model characterisation. More details about the generation and calibration of the image realisations can be found in Correia et al. (2023).

After 4DS interpretation, some geological features are incorporated in the geological model. Details of the interpreted 4DS insights are available in Maleki et al. (2021) and Maleki et al. (2022). The introduction of these 4DS insights into the model occurs as seismic trends through the geometrical

modelling technique for observed structural features, and the objects' modelling approach for the observed sand channels. The features are interpreted from seismic signal as with small transmissibility (e.g. faults or limits between sand channels) and the transmissibility of grid blocks is set as uncertain in the geostatistical generation of images. As a result, this second prior model ensemble, named in this work as Prior_4DS, differs to the Prior_no4DS ensemble only in the incorporation of 4DS data in the model characterisation. More details about the incorporation of 4DS features in the model can be found in Correia et al. (2023).

Data Assimilation Inputs

We consider different types of model uncertainties. Table 2 shows the minimum and maximum values of multiphase flow properties by means of Corey model for each rock type; Table 3, the well productivity and injectivity indexes (PI and II); and Table 4, the remaining model uncertainties. These bounds are applied in the ES-MDA by simple truncation if the property value falls outside these ranges during the data assimilation procedure. The prior distribution of all the uncertain attributes is defined as uniform.

The values of well PI and II define the relationship between total fluid (water and oil) rate and pressure drawdown for the production wells, and between water rate and drawdown for the injectors at the well start-up date, and is kept constant over the field life. For the 200 petrophysical realisations, properties that vary cell-by-cell throughout the grid, lower and upper bounds are imposed to avoid unphysical values during the data assimilation. The rock type realisations are not updated in DA.

Table 2: Minimum and maximum values of multiphase flow property uncertainties by rock type applied in the data assimilation.

Uncertain attribute	**RTP-1**		**RTP-2**		**RTP-3**		**RTP-4**	
	Min.	**Max.**	**Min.**	**Max.**	**Min.**	**Max.**	**Min.**	**Max.**
Connate water saturation (S_{wc})	0.70	0.92	0.60	0.75	0.325	0.475	0.05	0.20
Final water saturation ($S_w = 1-S_{or}$)	0.95	0.99	0.80	0.90	0.80	0.90	0.80	0.90
Irreducible oil saturation (S_{oirr})	0.02	0.05	0.02	0.07	0.02	0.07	0.02	0.07
K_{rw}[(1)] Corey exponent	2	5	2	5	2	5	2	5
K_{ro}[(2)] Corey exponent	2	5	2	5	2	5	2	5
K_{rg}[(3)] Corey exponent	2	5	2	5	2	5	2	5
K_{rl}[(4)] Corey exponent	2	5	2	5	2	5	2	5
K_{rw}[(1)] end-point	0.40	0.70	0.40	0.70	0.40	0.70	0.40	0.70
K_{ro}[(2)] end-point	0.60	0.80	0.60	0.80	0.60	0.80	0.60	0.80

[(1)] water-oil relative permeability; [(2)] oil-water relative permeability; [(3)] gas-liquid relative permeability; [(4)] liquid-gas relative permeability.

Table 3: Minimum and maximum values of well productivities and injectivities (STD. ft^3/day/psi) employed in the data assimilation.

	P10	P11	P2	P3	P5	P6	P8	P9	I1	I2	I5	I6
Min.	275.1	90.5	78.6	62.9	78.6	137.6	231.9	196.5	255.5	235.8	326.2	196.5
Max.	510.9	168.0	146.0	116.8	146.0	255.5	430.6	364.9	474.4	437.9	605.8	364.9

Table 4: Minimum and maximum values of petrophysical realisations and other uncertain attributes applied in the data assimilation.

Uncertain attribute	Min.	Max.
Net-to-gross spatial distribution (NTG)(1)	0	1
Porosity spatial distribution(1)	0	0.50
Horizontal abs. permeability spatial distribution (K_h)(1)	0	9,000
Vertical to horizontal abs. permeability (K_v/K_h) ratio	0.20	0.80
Horiz. abs. perm. anisotropy (n), being $K_{hI} = n \times K_h$; $K_{hJ} = (2 - n) \times K_h$	1.00	1.25
Pore compressibility (psi^{-1})	3.0×10^{-7}	3.0×10^{-5}
Original depth of water-oil contact (ft)	9,609.25	9,642.06
Analytical aquifer productivity index (ft^3/day/psi)	4,000	60,000
Initial volume of water in analytical aquifer (ft^3)	1.0×10^9	1.0×10^{13}

(1) *Petrophysical realisation with one value by grid block.*

The data assimilations are performed using the ES-MDA with 4 iterations, constant inflation factor and 200 models per ensemble, totalling 1,000 flow simulations per case (prior ensemble plus 4 assimilations). These definitions are based on the work of Emerick (2016), who obtained good results with these configurations.

The localisation definition for scalar and grid properties (petrophysical realisations) are based on the work of Soares et al. (2018), who defined the localisation regions based on streamlines for grid properties and applied a correlation matrix for the scalar ones. We applied a similar procedure as the work of Soares et al. (2018): from the simulation of the prior model ensemble, we chose a single model to analyse the streamlines. We decided to select this single model as the one with median field water production, since the water production presented the largest prior model misfits. The localisation was determined separately for the prior model ensemble with 4DS data (Prior_4DS) and the one without 4DS data (Prior_no4DS).

A total of 20 well data series are assimilated: Q_o and BHP for the 8 production wells, and BHP for the 4 injection wells. The observed data measurement errors are defined as a percentage of the data: 10% for oil rate with a minimum cut-off error of 25 m^3/day, and 2.5% for BHP.

For the 4D seismic data, we apply the observed maps of p-impedance changes between monitor three and baseline survey (m3/bs ratio). The settings of data preparation follow the same as Rosa et al. (2022): two maps, with the reservoir considered as two intervals: top-middle and middle-base of main sand (information on simulation grid zones in Table 1), a defined standard deviation value and an

exponential correlation with four-cell length of the simulation grid. We set the seismic standard deviation values of data error in a way that the prior normalized objective functions (OF) for well history and 4D seismic data are balanced. This is done in order to ensure that the contributions of both types of data in the DA process are similar (Rosa et al., 2022). Table 5 presents the normalized well history and 4D seismic OF for the prior model ensemble without 4DS (Prior_no4DS) and the one with it (Prior_4DS), which shows that both well history and 4DS data sets are reasonably well balanced.

Table 5: Mean normalized well data and 4DS objective functions for the prior model ensemble by case.

Model ensemble	Description	Norm. well history OF (mean)	Norm. 4DS OF (mean)
Prior_no4DS	Prior built without 4DS data	3.9226	4.3901
Prior_4DS	Prior built with 4DS data	4.4067	4.4158

Data Assimilation Cases

In order to evaluate the impact of 4DS data to the field production forecasting results at model characterisation and data assimilation steps, we perform three DA cases with different prior ensembles and different data sets assimilated (Table 6).

Table 6: List of simulation model ensembles, before and after data assimilation.

Case	Prior employed at DA	Data set assimilated	Colour code
Prior_no4DS	-	-	
Prior_4DS	-	-	
Post_no4DS	Prior built without 4DS	Well prod. and inj. data	
Post_4DSinDA	Prior built without 4DS	Well prod. and inj. data, and 4DS data	
Post_4DS	Prior built with 4DS	Well prod. and inj. data, and 4DS data	

Well PI and II Adjustment

For the adjustment of productivity and injectivity index of the wells, we switch the informed data to the simulator from well rates to bottom-hole pressure at the last producing or injecting date of the history period for each respective well, which is 2998 days for all the wells excepting P2 whose last producing date is day 2282.

Filtering

We apply the acceptance criterion for the well history data of 30 as cut-off value of the maximum $|NQDS_{HIST}|$ among all well functions (Q_w, BHP_p, etc.), meaning that a given model should have all the well functions with $|NQDS_{HIST}|$ lower than or equals 30 to pass the filter of well history data. This acceptance criterion is employed to the posterior model ensembles of all the data assimilation cases in Table 6.

The posterior ensembles from DA cases that utilise 4DS data (Post_4DSinDA and Post_4DS) are also filtered with regards to an acceptance criterion of 4DS. If a posterior ensemble model presents an MSE value (quantitative measure of 4DS matching quality) lower than its prior model, it passes the filter and proceeds to the final steps of validation and production forecasting. The remaining models are filtered out and are not applied in these final steps.

For Post_4DSinDA and Post_4DS cases, the posterior ensemble models must pass the acceptance criteria of both well history and 4DS criteria. The Post_no4DS ensemble employs just the well history data criterion at the filtering step, since this case does not apply 4DS data in the process. The prior ensembles are not subject to the filtering step and their results are shown on top of the three DA cases for comparison purposes, only.

Result Assessment

4D seismic data misfits

We analyse the misfit between the model ensemble results and the observed 4D seismic data in qualitative and quantitative means. At the former, we compare visually the mean model ensemble map of p-impedance ratio to the observed 4DS data at the two main sand reservoir intervals (top-middle and middle-base, with information on simulation grid zones in Table 1). At the latter, we employ the mean square error (MSE) of the entire reservoir region, similarly to Santos et al. (2022), over the middle-base interval.

We evaluate the misfits between the 4DS observed data and model results in two separate time periods: history (with the first monitor to base ratio, m3/bs, which is assimilated) and validation (with the second monitor to base ratio, m5/bs, which is not assimilated).

Well production and injection data misfits

For the evaluation of well production and injection data misfits between observed data and simulated results, we employ the NQDS (Normalized Quadratic Deviation with Sign) indicator for quantitative analysis and, additionally, well production and injection curves to complement it. Equations 3 to 6 present the steps to obtain the NQDS value for each well data time series (well functions) (Q_o, BHP_p, etc.). This indicator was firstly presented by Almeida et al. (2014), Avansi and Schiozer (2015) and Silva et al. (2015), and later by Avansi et al. (2016) and Maschio and Schiozer (2016).

$$LD = \sum_{i=1}^{N_{obs}} (Sim_i - Obs_i) \qquad (3)$$

$$QDS = \frac{LD}{|LD|} \sum_{i=1}^{N_{obs}} (Sim_i - Obs_i)^2 \qquad (4)$$

$$AQD = \sum_{i=1}^{N_{obs}} (Tol \times Obs_i + C)^2 \qquad (5)$$

$$NQDS = \frac{QDS}{AQD} \qquad (6)$$

N_{obs} is the number of observed data in a given well data time series. *Tol* is a tolerance defined as a percentage of the observed data. *C* is a constant used to avoid excessive weight for very small data values. Similar to the analysis of model misfits with regards to the 4D seismic data, we use the NQDS indicator to quantify the misfit from well data observations and model results in two separate time periods: history ($NQDS_{HIST}$), in which the data is assimilated, and validation ($NQDS_{VALID}$), in which the data is used for benchmark purposes. Table 7 shows the *Tol* and *C* values applied for each well data time series (well function).

Table 7: Parameters utilized in the calculation of $NQDS_{HIST}$ and $NQDS_{VALID}$ indicators for each well data time series.

Indicator	Parameter	Well data time series						
		Q_l	Q_o	Q_w	Q_g	BHP_p	BHP_i	Q_{wi}
$NQDS_{HIST}$	*Tol*	5%	10%	10%	15%	2.5%	2.5%	5%
$NQDS_{HIST}$	*C*	0	0	1 m^3/day	0	0	0	0
$NQDS_{VALID}$	*Tol*	10%	10%	10%	15%	2.5%	2.5%	10%
$NQDS_{VALID}$	*C*	0	5 m^3/day	5 m^3/day	0	0	0	0

We adopted a *C* constant value different than zero for Q_o and Q_w of $NQDS_{VALID}$ because P2 well operates at a very small production rate of oil and water for a significant portion of the validation period of time.

Production Forecasting under Uncertainties

After the data assimilation, adjustment of well productivities and injectivities, filtering of posterior model ensembles with dynamic data (well production and injection data, and 4DS data) of history period (between day 1 and 2298) and simulation under validation conditions (from day 2299 to 2359), the models undergo through the production forecasting period between day 2360 and 7763.

In this work, we evaluate the production forecasting results in terms of the future cumulative oil production ($N_{p,fut}$) (remaining oil production) by employing the reference day of 2206 days, which corresponds to the date when the field decision is taken in the project. We apply the same operating constraints (platform capacity and well operation) for all the simulation model ensembles.

RESULTS AND DISCUSSIONS

Before presenting the results obtained with the different data assimilation cases depicted in "APPLICATION – Data assimilation cases" section, it is important to mention some aspects of the computational time spent for practical applications.

For the Post_4DS case, the median simulation run time for each model of the ensemble was approximately 60 minutes using 10 CPU. The median elapsed time for each iteration of the analysis step of data assimilation, which includes the processing of the grid model properties and model errors,

was about 20 hours.

Considering the use of a simulation cluster with 100 CPU (10 groups of 10 CPU), for the entire Post_4DS case comprising the simulation of prior ensemble, the 4 ensembles for the iterations and the ensemble after well PI and II adjustment, totalling 6 ensembles, it took: (1) a simulation run time in the magnitude order of 5 days (60 min/model/group of CPU x (1/10 groups of CPU) x 200 models/ensemble x 6 ensembles), and (2) processing of the analysis step of data assimilation iterations in the magnitude order of 4 days (20 hours/iteration x 4 iterations + 20 hours/ensemble x 1 ensemble after well PI and II adjustment). Considering the model simulations performed in a cluster with parallel computing as employed in this work, one may say that the computational time to obtain the results is affordable.

Model Properties

Scalar attributes

Figure 4 shows a boxplot of the scalar attributes that present more differences among the posterior model cases. The well productivity index of P5 (Figure 4a) shows a progressive increase with the utilisation of 4DS data from Post_no4DS to Post_4DSinDA and Post_4DS. This difference in the PI of P5 is related to the different effect of grid property updating with introduction of 4DS data, especially the horizontal absolute permeability. The mean maps of this property in P5 well region (Figure 3 and Figure 5) support this analysis, with the highest horizontal absolute permeability occurring for the Post_no4DS case, and the lowest one for Post_4DS.

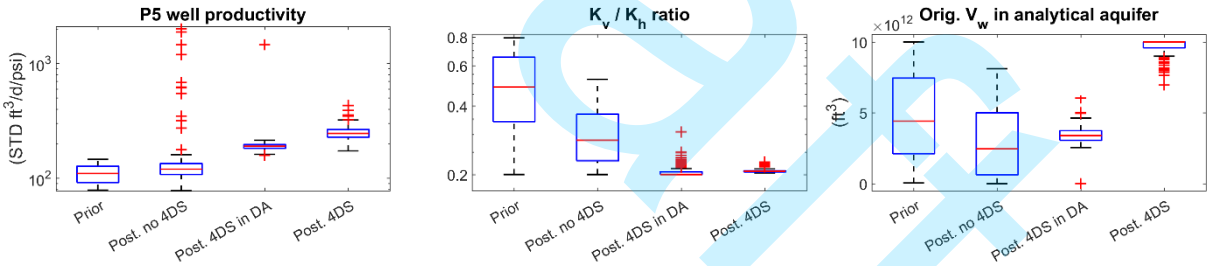

(a) (b)(c)

Figure 4: Distribution of scalar model uncertainties for prior and posterior model ensembles: (a) P5 well productivity, (b) K_v/K_h ratio, and (c) original volume of water in the analytical aquifer.

The vertical to horizontal absolute permeability (K_v/K_h ratio) in Figure 4b shows a similar behaviour with the introduction of 4DS data for Post_4DSinDA and Post_4DS cases. This scalar property is one of the most impacting the fluid saturation changes, and it shows consistency of the 4DS data assimilation across the cases whether employing or not 4DS in the prior model ensemble. The uncertainty of this property was much diminished with just assimilating 4DS data (from Prior to Post_4DSinDA), what demonstrates a strong impact of 4DS data assimilation.

For the original volume of water (V_w) in the analytical aquifer (Figure 4c), we can see that just assimilating 4DS data (Post_4DSinDA case) resulted in posterior values within the interval of values of

Post_no4DS but it reduced a lot the uncertainty of this model property. At the other side, Post_4DS led to higher values of the original V_w. It is important to mention that this is commonly a difficult property to be estimated, and the introduction of 4DS data in the model characterisation step shows a big impact for this case study.

Grid attributes

Figure 5 shows the mean and standard deviation of effective porosity and horizontal absolute permeability at K-43 layer of each model ensemble. This layer is an intermediate layer in the middle-base interval of main sand body, where most of the changes in the fluid flow caused by production and injection occur.

The property variability (standard deviation) of posterior model ensembles decreases in relation to the prior ones, what is an expected result of the ES-MDA application. It calls our attention the strong reduction in effective porosity variability for the Post_no4DS case in the central-east area of the map. This is associated with the lower effective porosity obtained for this case in comparison to the other posterior ensembles. As it occurs around several production and injection wells (P2, P3, P6, I2 and I5 wells), we can explain this region in Post_no4DS as the property result that could best fit the well history data when no 4DS data is employed.

Both effective porosity and horizontal absolute permeability change significantly with the joint data assimilation of 4DS and well history (Post_4DSinDA) in relation to DA of just well history (Post_no4DS): the effective porosity increases substantially overall, while the horizontal absolute permeability decreases in the central-west area of the reservoir.

When 4DS is employed in both model characterisation and data assimilation (Post_4DS), the variability of effective porosity and horizontal absolute permeability in posterior compared to prior diminishes less than just assimilating it (Post_4DSinDA), especially near the borders of the grid. This indicates that the incorporation of 4DS data in the model characterisation helps to preserve the property variability at locations that are far from the wells, provided that Prior_no4DS and Prior_4DS ensembles do not present significant changes in the property variability overall between each other.

4D Seismic Data Misfits

Figure 6 shows the observed p-impedance ratio between each of the monitor and base surveys (m3/bs and m5/bs) at top-middle and middle-base of main sand interval on the first line, and the respective mean maps of each model ensemble on the following lines.

When we compare the model ensembles to the observed maps, we can see the great impact of 4DS to the improvement of model results. The posterior case with 4DS in both model characterisation and data assimilation (Post_4DS) agrees more with the observed maps overall, mainly because the DA of 4DS without its use in characterisation (Post_4DSinDA) led to a softening anomaly above P5 well location in both m3/bs and m5/bs ratios (arrows A in Figure 6). This softening anomaly is not present in the observed signal. The posterior case without 4DS (Post_no4DS) also does not show the softening

anomaly around P5 and P6 region that is observed at the middle-base interval (arrows B), while Post_4DS and Post_4DSinDA do.

We can take some conclusions on a sand channel that was inserted in the Prior_4DS ensemble from the interpretation of geological features identified through analysis of the 4DS observed signal. This sand channel takes water from the bottom aquifer to P9 well and its margins were modelled inserting low abs. permeability in the Prior_4DS (arrows A in Figure 5). The p-impedance ratio of both m3/bs and m5/bs at the middle-base interval shows the effect of this identified sand channel at the observed signal and the prior ensemble built with 4DS (arrows C in Figure 6). The data assimilation helped improving this channel delineation as we can see in the m3/bs map of Post_4DS and it is more evident in the m5/bs map (arrows D in Figure 6). We believe that this sand channel inserted in the model characterisation also prevented the softening anomaly above P5 in the Post_4DsinDA ensemble (use of prior built without application of 4DS data) as discussed in the previous paragraph and indicated by the arrows A in Figure 6, from appearing in Post_4DS (use of prior with 4DS data).

Another clear anomaly that is not present in the observed signal but appears on the model results is the softening anomaly on the east region in the top-middle interval of both m3/bs and m5/bs of Post_no4DS (arrows E in Figure 6). This is associated with the lower effective porosity of this case in relation to the other model ensembles (Figure 5). As this anomaly is not present in the Prior_no4DS neither the Post_4DSinDA, one can conclude that it was an artefact caused by the assimilation of well history data without 4DS data.

As a conclusion of the qualitative analyses of p-impedance ratios, the combined application of 4DS data in model characterisation and data assimilation was important to obtain model ensembles with better fit of the observed 4DS signal.

Figure 7 shows the mean square error (MSE) of middle-base interval of both m3/bs and m5/bs p-impedance ratios, for each model ensemble. The quantitative results of MSE corroborates with the qualitative analyses of 4DS maps, which indicated that the Post_4DS model ensemble resulted in closer results to the obs. signal for both m3/bs and m5/bs in relation to all model ensembles. This is evidenced by the lowest values of MSE for Post_4DS. We can also depict from Figure 7 that the MSE variation reduced more for this case than the posterior ensembles that do not incorporate 4DS data in the model characterisation (Post_no4DS and Post_4DSinDA). This occurs even though Prior_4DS shows bigger variation than Prior_no4DS. Thus, the integrated DA of well history and 4DS data using the prior ensemble built with 4DS (Prior_4DS) was responsible for substantially diminishing the MSE values. Another observation is the MSE change from m3/bs to m5/bs, with Post_4DS maintaining the low values, what indicates good validation results in terms of 4DS data (remembering the m5 was not assimilated). The MSE of Post_4DSinDA had a relative increase in m5/bs due to the softening anomaly above P5 well location in the map as it was previously discussed (arrows A in Figure 6).

As a sum, the MSE results indicate that, even though the Prior_no4DS and Prior_4DS show similar errors for both m3/bs and m5/bs p-impedance ratios, the model characterisation step was very impactful on posterior results when we compare Post_4DSinDA and Post_4DS cases.

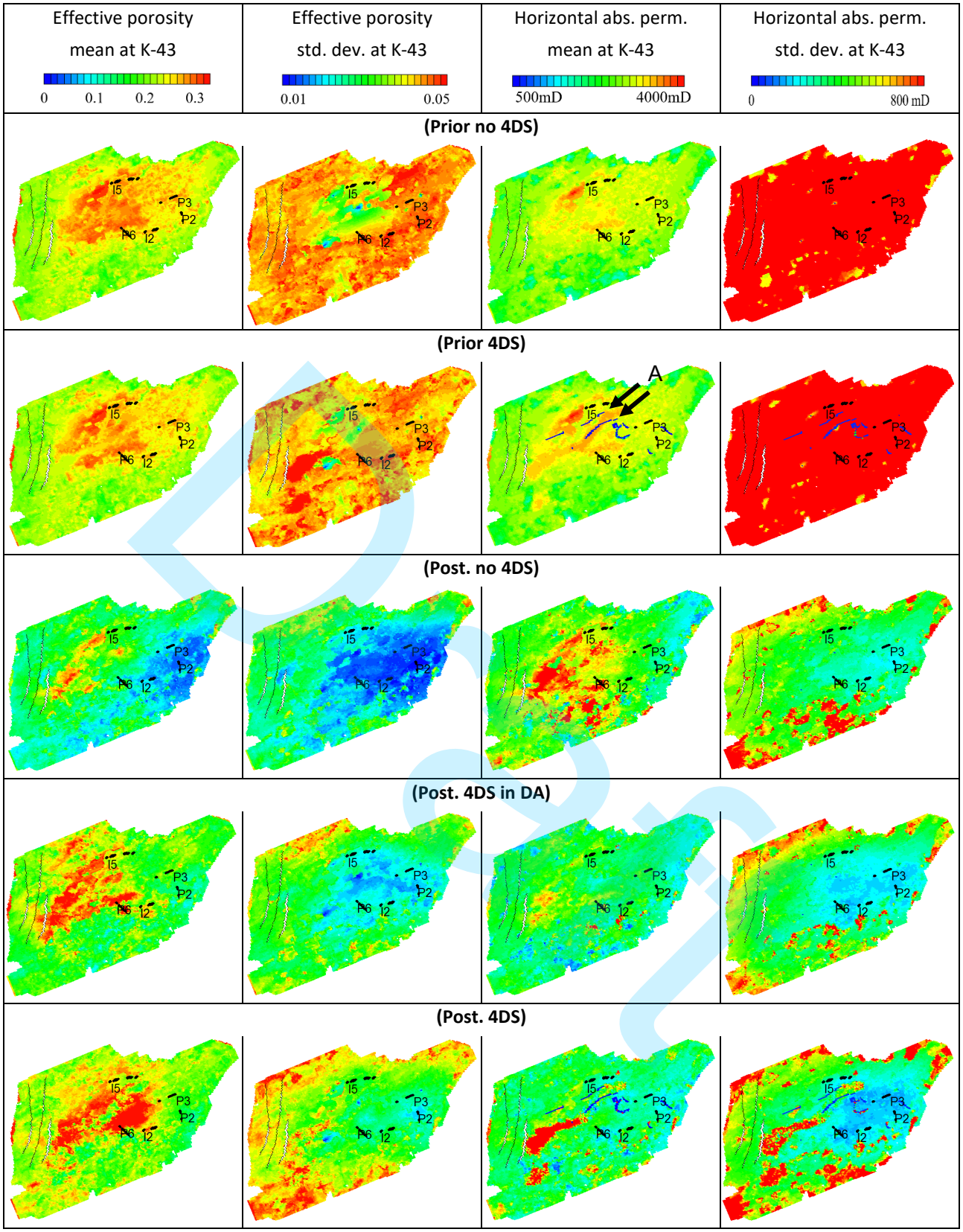

Figure 5: Mean and standard deviation map at K-layer 43 for prior and posterior model ensembles.

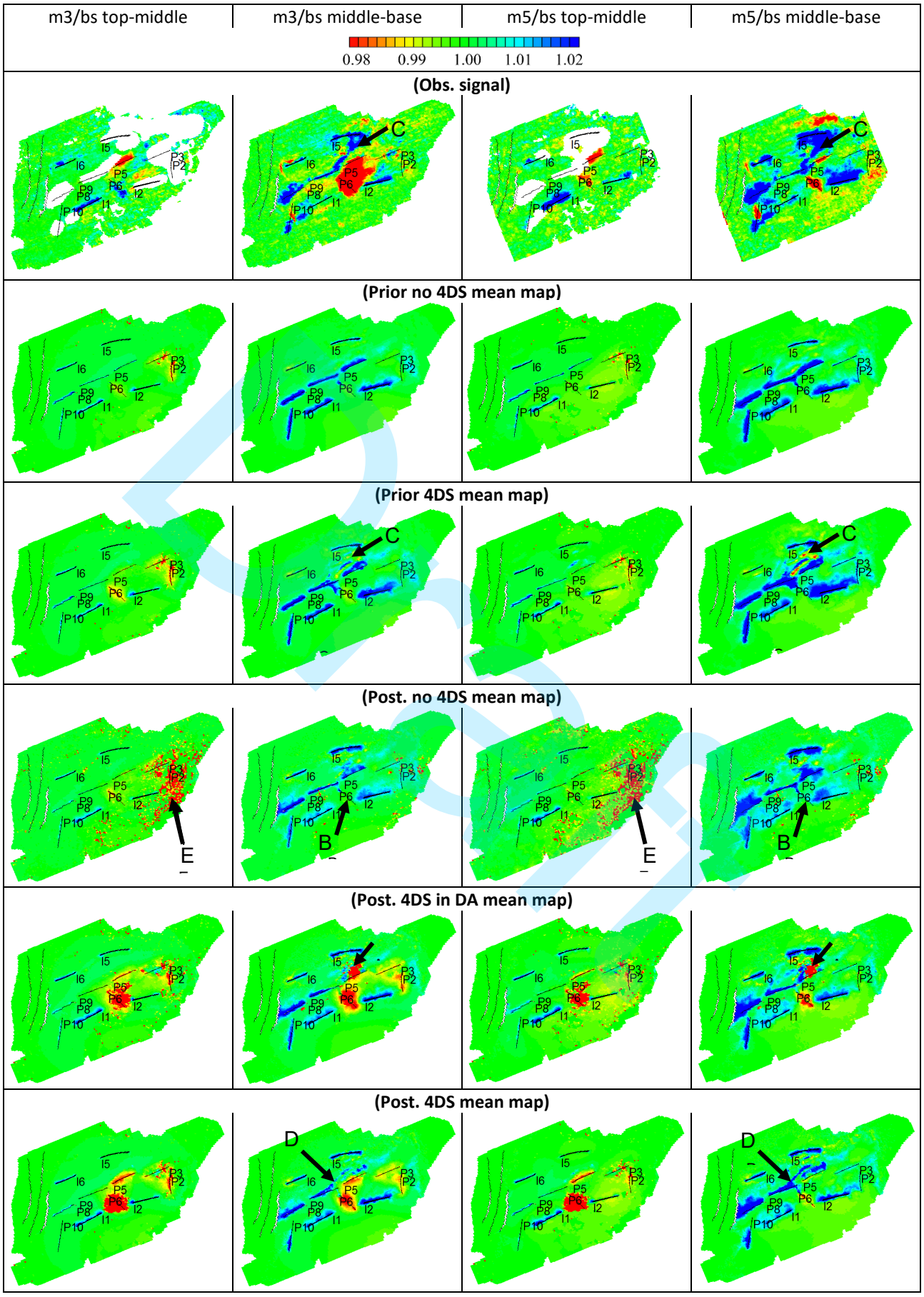

Figure 6: m3/bs and m5/bs p-impedance ratios for top-middle and middle-base intervals.

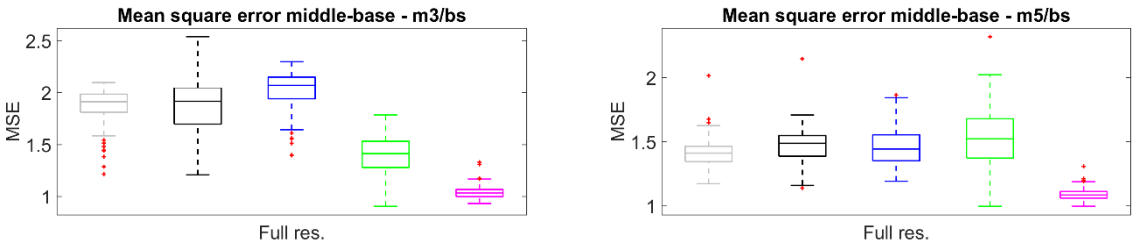

Figure 7: Mean square error (MSE) between the observed signal and each model ensemble calculated over the middle-base interval for Prior_no4DS (grey colour), Prior_4DS (black), Post_no4DS (blue), Post_4DSinDA (green) and Post_4DS (magenta): (a) m3/bs, and (b) m5/bs p-impedance ratios.

Well Production and Injection Data Misfits

The informed data to the simulation during the history period (Q_l for producers and Q_{wi} for injectors) is honoured by all models for all the wells, so $NQDS_{HIST}$ indicator equals zero for Q_l and Q_{wi}. This indicator is shown in Figure 8 for all the other well functions (BHP_p, BHP_i, Q_o, Q_w and Q_g). We can see that most of them do not differ significantly among the posterior model ensembles, having all cases general good results in terms of well matching.

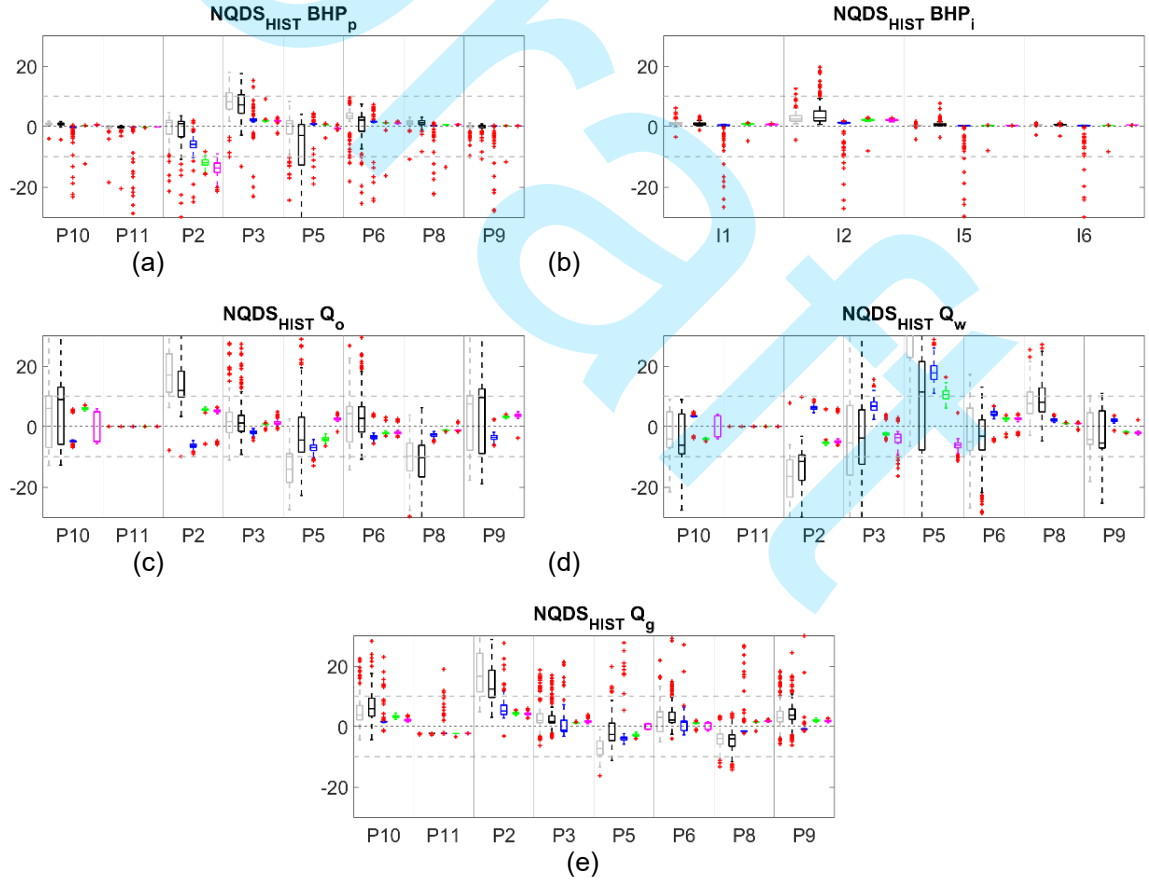

Figure 8: Normalized quadratic deviation with sign on history period ($NQDS_{HIST}$) for Prior_no4DS (grey colour), Prior_4DS (black), Post_no4DS (blue), Post_4DSinDA (green) and Post_4DS (magenta).

Some exceptions are P2 and P5 wells. The bottom-hole pressure of P2 decreases progressively from Post_no4DS to Post_4DSinDA and Post_4DS, becoming more distant of the history data series. This occurs because the horizontal absolute permeability in the region of P2 well is progressively lower on this case order (Figure 5), and its well productivity was not able to account for this effect. The P5 water production rate and, as a consequence, its oil rate are closer to the history data (smaller value of $|NQDS_{HIST}|$) for Post_4DS case due to the incorporation of 4DS data in the prior model ensemble. This is evidenced by the smaller $|NQDS_{HIST}|$ values of Prior_4DS in relation to Prior_no4DS for Q_o and Q_w of P5 well. Figure 9 shows the Q_o and BHP curves of P5 well for visualization purposes of the $NQDS_{HIST}$ indicator.

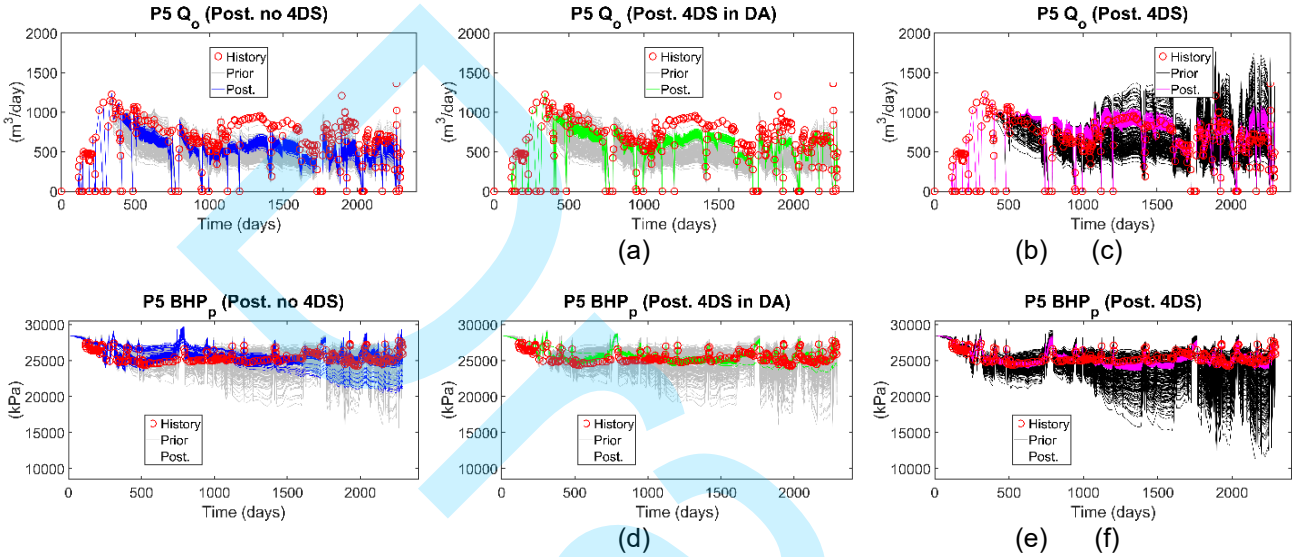

Figure 9: Oil production rate (Q_o) and bottom-hole pressure (BHP_p) curves of P5 well during history period for posterior ensembles on top of their prior ensembles: Post_no4DS (blue), Post_4DSinDA (green) and Post_4DS (magenta).

Filtering with Well History and 4DS Data

Figure 10a presents the distribution of maximum $|NQDS_{HIST}|$ among all the well functions before the filtering step with well history data, which is employed to screen out the worst models based on this type of data. The more to the left the curve is, the lower the maximum $|NQDS_{HIST}|$ by model, and the more ensemble members are to be filtered in for validation and production forecasting applications.

The cases with 4DS (Post_4DSinDA and Post_4DS) present a distribution more to the left than the case without 4DS (Post_no4DS), indicating that 4DS data actually improved the well matching for filtering purposes. In addition, 10% of the models from Post_no4DS case shows a maximum $|NQDS_{HIST}|$ value much higher than the rest of the ensemble (right most part of the blue curve in Figure 10a). The well functions with highest $|NQDS_{HIST}|$ for these 10% of models from this case are Q_g and BHP_p in general, as it can be depicted from Figure 8. This happens because of the lower effective porosity for Post_no4DS in comparison to the other cases (first column of Figure 5), which caused lower BHP_p (lower $NQDS_{HIST}$ for BHP_p) and, as a consequence, high Q_g (high $NQDS_{HIST}$ for Q_g) due to free gas being produced.

The data assimilation of 4DS information improved the distribution, since the Post_4DSinDA case presents a curve with lower values of maximum $|NQDS_{HIST}|$ than Post_no4DS case (Figure 10a), having both utilized the same prior model ensemble (Prior_no4DS). The incorporation of 4DS data into the model characterisation did not impact substantially the posterior results, as the Post_4DS shows a similar distribution to Post_4DSinDA. It is important to mention that the difference between these two model ensembles is the incorporation of 4DS data in the model characterisation step, which does not intend to improve the well matching results. Therefore, this is not an unexpected result.

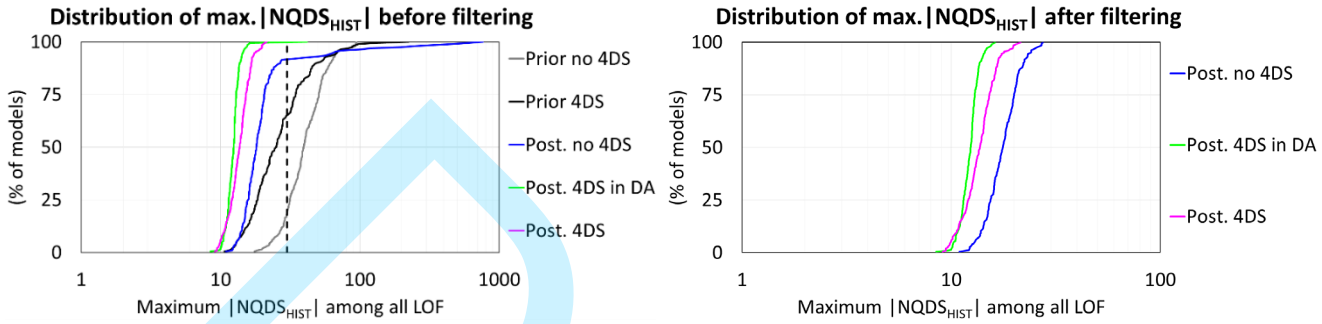

Figure 10: Distribution of maximum $|NQDS_{HIST}|$ among all well functions for each model ensemble (a) before the filtering step applied with well history data, with the cut-off for validation and production forecasting applications represented by the vertical dashed line, and (b) after the filtering step applied with well history data.

The models from the posterior model ensembles with the maximum $|NQDS_{HIST}|$ value lower than 30 were filtered in (well history data criterion) for validation and production forecasting applications, representing 91.5% of models for Post_no4DS, 99.5% for Post_4DSinDA and 100% for Post_4DS. Figure 10b shows the distribution of maximum $|NQDS_{HIST}|$ among all the well functions for the posterior model ensembles after the filtering with well history data.

Figure 11 presents the cross plot of mean square error (MSE) of middle-base interval of m3/bs between the prior and posterior models for each data assimilation case. We can see that all posterior ensemble members of the case that applied 4DS data in model characterisation and DA (Post_4DS) show lower MSE than the prior, confirming that the data assimilation reduced the 4DS error for all models. As a result, no models were filtered out with regards to 4DS data for this case. The case that employed 4DS only at DA (Post_4DSinDA) shows 7 posterior models with MSE higher than their respective prior, so these models were filtered out. The case without 4DS (Post_no4DS) shows many posterior models with higher MSE than their prior. However, the filtering step with regards to 4DS is not applied to this case because it does not consider any 4DS information along the process.

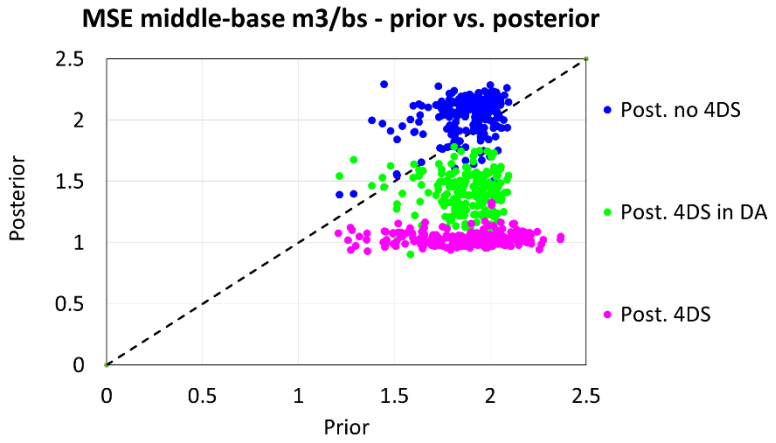

Figure 11: Mean square error (MSE) between the observed signal and each model ensemble calculated over the middle-base interval for m3/bs with the prior result in the horizontal axis and posterior in the vertical axis for each data assimilation case.

Figure 12 shows the cross plot between the 4DS metric employed in the filtering (MSE of middle-base interval of m3/bs) and the well history metric employed (maximum $|NQDS_{HIST}|$ among all local objective functions) for the case Post_4DSinDA. We can see the only model previously filtered out by the well history criteria (Figure 10a) in red and the seven models filtered out by the 4DS criteria in black, totalling 8 models filtered out for this case. We do not show the Post_4DS case because all the models can pass the acceptance criteria of both 4DS and well history and do not present the Post_no4DS because the 4DS data is not utilized along the process for this case.

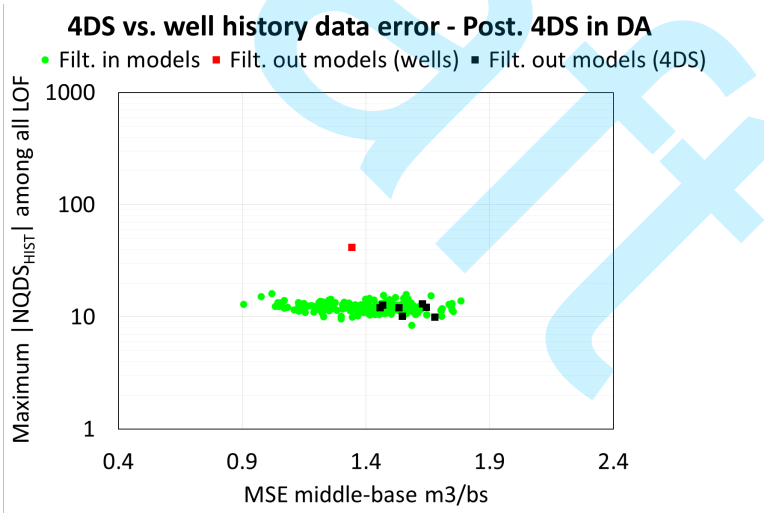

Figure 12: Filtering criteria applied to Post_4DSinDA case, with the 4DS error in the horizontal axis and the well history data error in the vertical axis.

Predictive capacity of the models

During the validation period, the bottom-hole pressure of all producers and injectors are used as boundary condition informed to the simulator. Since all DA cases present good well matching overall

("RESULTS AND DISCUSSIONS - Well Production and Injection Data Misfits" section), $NQDS_{VALID}$ is zero for BHP.

Figure 13 shows the boxplots of $NQDS_{VALID}$ for Q_l, Q_{wi} and Q_o. In addition to the posterior models that were filtered in from each ensemble, we also include all the models from the prior ensembles for comparison purposes. In general, Post_no4DS resulted in lower misfits than the posterior cases with 4DS, but not a significantly big difference. It is important to note that no 4DS data is being employed to evaluate the predictive capacity of the models and, as a consequence, the capacity of the model ensembles that employed 4DS in the process (Post_4DSinDA and Post_4DS) cannot be fairly compared to Post_no4DS. We should consider that the Post_no4DS ensemble was developed in order to specifically produce close results to the well production and injection data and, for this reason, such small differences observed in the predictive capacity do not represent a relevant advantage for Post_no4DS in relation to Post_4DSinDA and Post_4DS. Figure 14 and Figure 15 show, respectively, the P5 and I2 well curves for visualization purposes of the $NQDS_{VALID}$ indicator.

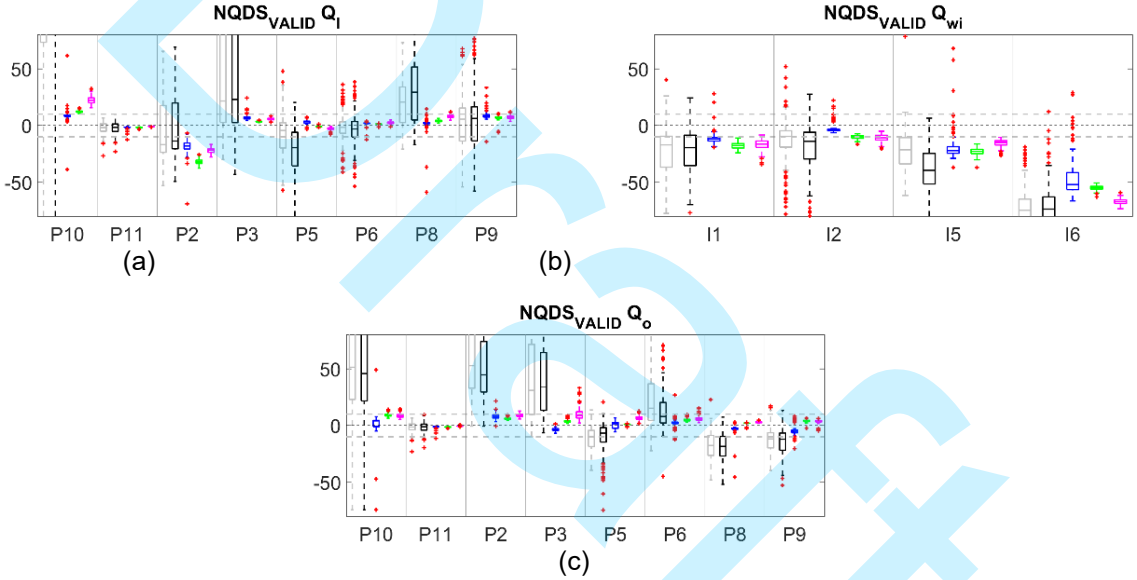

Figure 13: Normalized quadratic deviation with sign on validation period ($NQDS_{VALID}$) for Prior_no4DS (grey colour), Prior_4DS (black), Post_no4DS after filtering (blue), Post_4DSinDA after filtering (green) and Post_4DS after filtering (magenta): a) liquid production rate (Q_l), b) water injection rate (Q_{wi}) and c) oil production rate (Q_o).

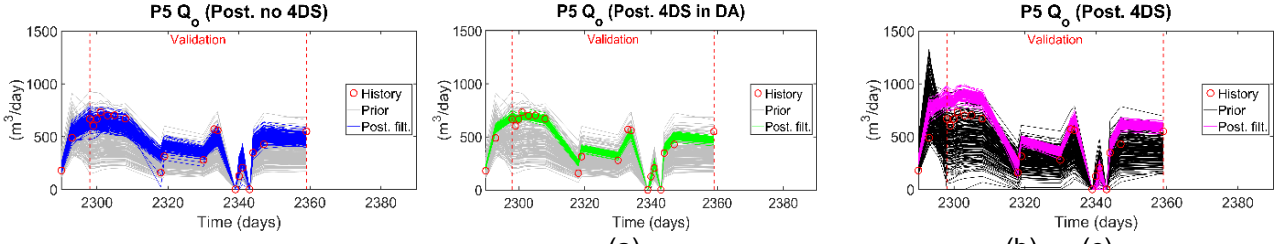

Figure 14: Oil production rate (Q_o) curves of P5 well during validation period for posterior ensembles after filtering on top of their prior ensembles: a) Post_no4DS (blue), b) Post_4DSinDA (green) and c) Post_4DS (magenta).

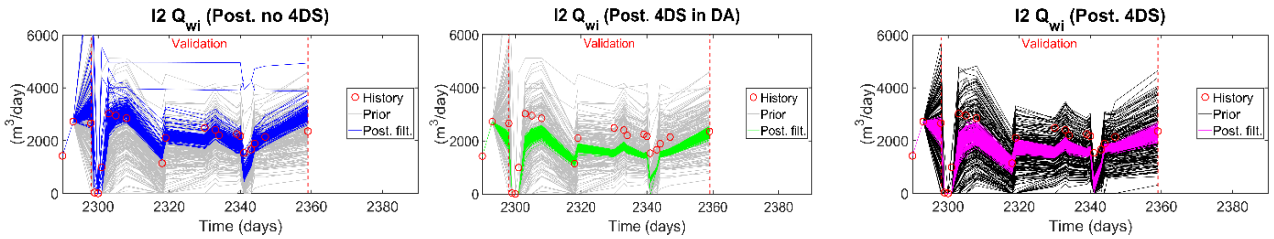

Figure 15: Water injection rate (Q_{wi}) curves of I2 well during validation period for posterior ensembles after filtering on top of their prior ensembles: a) Post_no4DS (blue), b) Post_4DSinDA (green) and c) Post_4DS (magenta).

Production Forecasting under Uncertainties

Figure 16 shows the future cumulative oil production (remaining oil production) curves for each model ensemble from day 2206 to 7763. We present, once again, all the models from prior ensembles in addition to the posterior models that were filtered in, for comparison purposes. We can see that the case that applied 4DS data only at data assimilation (Post_4DSinDA) provides distinct curves of the posterior without 4DS (Post_no4DS), with more optimistic oil production, even though these cases employ the same prior model ensemble. The case that incorporated 4DS data at model characterisation and DA (Post_4DS) present more variability than Post_4DSinDA. This appears to be related to the higher variability of effective porosity and horizontal absolute permeability near the grid borders of the former compared to the latter, as it was discussed previously, at “RESULTS AND DISCUSSIONS – Model Properties - Grid attributes” section.

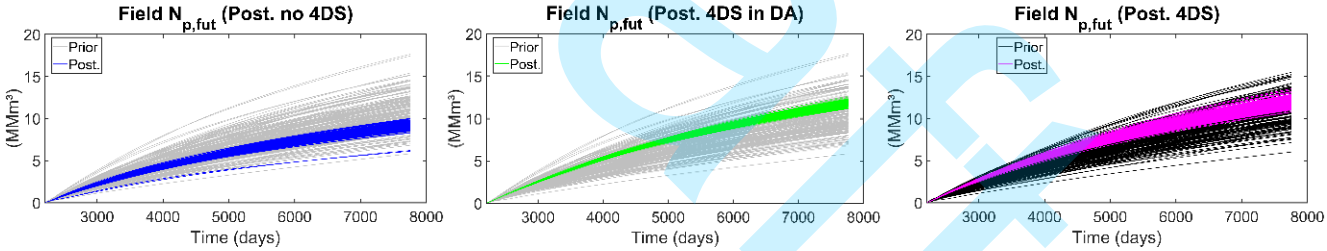

Figure 16: Future cumulative oil production after filtering on top of their prior ensembles: a) Post_no4DS (blue), b) Post_4DSinDA (green) and c) Post_4DS (magenta).

Figure 17 shows the distribution of final $N_{p,fut}$ (at the day 7763) for each posterior model ensemble. The difference between the Post_4DSinDA case and Post_4DS is not much significant, with the latter presenting more variable risk curve. The case that does not apply 4DS in neither data assimilation nor model characterisation (Post_no4DS) has a difference of approximately 23% in the mean remaining field oil production compared to the cases with 4DS, what is a huge difference: 9.178 MMm^3 STD. for Post_no4DS, 11.757 for Post_4DSinDA and 11.995 for Post_4DS.

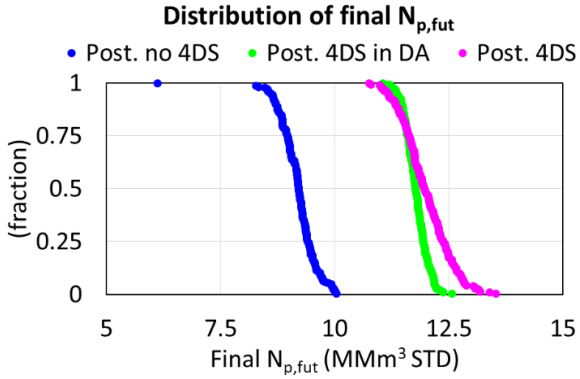

Figure 17: Future cumulative oil production at the day 7763 (final $N_{p,fut}$) (remaining oil production) for the posterior model ensembles after filtering: Post_no4DS (blue), Post_4DSinDA (green) and Post_4DS (magenta).

The difference in in the mean remaining field oil production between Post_no4DS and the cases with 4DS (Post_4DSinDA and Post_4DS) is associated with the original volume of oil in place (VOIP) (Figure 18), which shows the Post_no4DS case with the lowest values of VOIP, and some model properties such as the original V_w in the analytical aquifer (Figure 4c), denoting more energy capacity of the analytical aquifer for Post_4DS in relation to the other cases.

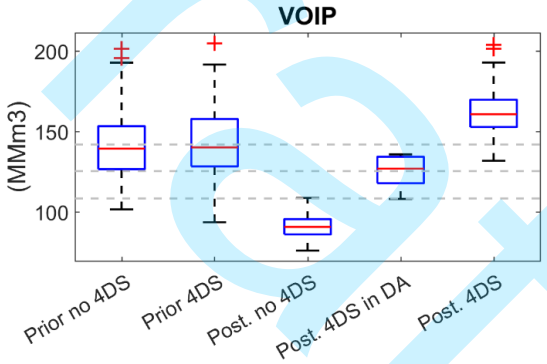

Figure 18: Distribution of original volume of oil in place for prior, and posterior model ensembles after filtering.

The final production forecasting results indicate a strong impact of 4DS data assimilation in the process compared to the non-application of 4DS, and a secondary effect of 4DS data incorporation in the model characterisation for this case study. In terms of overall quality of model results, though, the Post_4DS case is the best choice to take field decisions because it yields the best model fit in relation to the observed dynamic data (well history and 4DS) as it was discussed in the previous items.

CONCLUSIONS

In this work, we proposed and applied a methodology to a real field that evaluates the relative changes obtained in the field production forecasting among cases with and without the incorporation of 4DS data, by demonstrating a data assimilation study integrating 4DS and well history data.

The model misfits to the well production and injection data that was assimilated (history data) did not change significantly among the cases. In general, all the cases presented good results in terms of well matching. The cases that employed 4DS data resulted in a higher number of models passing through the filtering step (with history and 4DS data) for the final steps of validation and production forecasting. Some modifications introduced in model characterisation with 4DS data improved the misfits of multiphase flow rates of P5 well in relation to the case without 4DS data. At the other side, the bottom-hole pressure of P2 well resulted in lower misfits for the case without 4DS due to the update of horizontal absolute permeability being more able to adjust this well function than the cases with 4DS.

The qualitative analysis of 4DS assimilated data showed closer maps, in relation to observed data, for the cases that assimilated 4DS data than the case without 4DS, as expected. The best results occurred for the case with 4DS data in the model characterisation due to the sand channel that was modelled, taking water from the bottom aquifer to P9 well. The quantitative analysis by means of the mean square error corroborates with the qualitative analysis making it less subjective.

After the data assimilation, we successfully performed the model validation by employing a period of well production and injection data, and one 4D seismic monitor survey for this purpose. We obtained satisfactory results for all the cases in both qualitative and quantitative means. The best validation results of well data occurred for the case without 4DS, and the best results of 4DS data, for the case with 4DS incorporated in model characterisation and DA, as expected.

The case without 4DS data provided significantly more pessimistic field oil production forecast than the cases with 4DS, with an approximate difference of 23% in the remaining field oil production. This is explained by the smaller volume of original oil in place due to lower effective porosity and weaker analytical aquifer support for the former in relation to the latter. The incorporation of 4DS data in model characterisation impacted the final oil production forecast at lower degree than the data assimilation.

In sum, the application of 4DS in both model characterisation and data assimilation steps brought value to the final uncertainty reduction results. The posterior model ensemble with 4DS data in model characterisation and DA provided lower model misfits overall to both well and 4D seismic data than the other cases by considering history and validation periods. The remaining field oil production was significantly lower for the case that did not apply 4DS data in relation to the cases that did. Although the distribution of final cumulative field oil production did not differ much between the case with 4DS just in DA and the case with 4DS in both characterisation and DA, some model properties such as porosity and abs. permeability at some regions of the reservoir did. This may be of significant impact to infill drilling positioning. In addition to the lowest model misfits of the case applying 4DS along the entire process, this observation confirms that it is the best choice for application at field production forecasting studies.

ACKNOWLEDGMENTS

This work was carried out in association with the Project registered under number 20372-9 ANP as the “Development of integration between reservoir simulation and seismic 4D - Phase 2” (University of

Campinas [UNICAMP]/Shell Brazil/ANP) funded by Shell Brasil Petróleo Ltda. under the R&D ANP levy as the “Investment Commitment to Research and Development.” The authors are grateful for the support of the Centre for Energy and Petroleum Studies (CEPETRO-UNICAMP/Brazil), the Department of Energy (DE-FEM-UNICAMP/Brazil), the Research Group in Reservoir Simulation and Management (UNISIM/UNICAMP/Brazil), and Energi Simulation. In addition, a special thanks goes to Alexandre A. Emerick (Petrobras) for providing the EHM tool to UNISIM, Daiane Rossi Rosa for the technical discussions and 4D seismic assimilation inputs, Juliana Carvalho Maia Santos for the technical discussions and for providing the petro-elastic model (PEM), Manuel Correia for providing the petrophysical realisations, and Masoud Maleki for the 4D seismic features inserted at petrophysical realisations. The authors would also like to thank SLB and CMG for software licenses.

Reference

Almeida, F.L.R.; Gomes, A.D.; Schiozer, D.J., 2014. A New Approach to Perform a Probabilistic and Multi-objective History Matching, Paper number SPE-170623-MS, SPE Annual Technical Conference and Exhibition, Amsterdam, The Netherlands. DOI: https://doi.org/10.2118/170623-MS.

Almeida, F.L.R., Formentin, H.N., Maschio, C., Davolio, A., Schiozer, D.J., 2018. Influence of Additional Objective Functions on Uncertainty Reduction and History Matching. Paper number: SPE-190804-MS, SPE Europec featured at 80th EAGE Conference and Exhibition, Copenhagen, Denmark, June 2018. DOI: https://doi.org/10.2118/190804-MS.

Avansi, G.D., Schiozer, D.J., 2015. A New Approach to History Matching Using Reservoir Characterization and Reservoir Simulation Integrated Studies. Paper number: OTC-26038-MS, Houston, Texas. DOI: https://doi.org/10.4043/26038-MS.

Avansi, G.D., Maschio, C., Schiozer, D.J., 2016. Simultaneous history-matching approach by use of reservoir-characterisation and reservoir-simulation studies. SPE Reservoir Eval. Eng. 19 (4), 694–712. DOI: https://doi.org/10.2118/179740-PA.

Brouwer, D.R., Nævdal, G., Jansen, J.D., Vefring, E.H., Van Kruijsdijk, C.P.J.W., 2004. Improved Reservoir Management through Optimal Control and Continuous Model Updating. Paper number: SPE-90149-MS, SPE Annual Technical Conference and Exhibition, Houston, Texas, pp. 26–29. DOI: https://doi.org/10.2118/90149-MS.

Correia, M., Maleki, M., Silva, F.B.M., Davolio, A., Schiozer, D.J., 2023. Integrated Approach to Improve Simulation Models in an Deepwater Heavy Oil Field with 4D seismic monitoring. Petroleum Geoscience: *in press*. DOI: https://doi.org/10.1144/petgeo2022-048.

da Nobrega, D.V., de Moraes, F.S., Emerick, A.A., 2018. Data assimilation of a legacy 4D seismic in a brown field. J. Geophys. Eng. 15, 2585–2601. DOI: https://doi.org/10.1088/1742-2140/aadd68.

De Souza, R.M., Machado, A.F., Munerato, F.P., Schiozer, D.J., 2010. Iterative history matching technique for estimating reservoir parameters from seismic data. SPE EUROPEC/EAGE Annual Conference and Exhibition. OnePetro. DOI: https://doi.org/10.2118/131617-MS.

Emerick, A.A., Reynolds, A.C., 2013a. History-matching production and seismic data in a real field case using the ensemble smoother with multiple data assimilation. SPE Reservoir Simulation Symposium. The Woodlands, Texas, USA. DOI: https://doi.org/10.2118/163675-MS.

Emerick, A.A., Reynolds, A.C., 2013b. Ensemble smoother with multiple data assimilation. Comput. Geosci. 55, 3–15. DOI: https://doi.org/10.1016/j.cageo.2012.03.011.

Emerick, A.A., 2016. Analysis of the performance of ensemble-based assimilation of production and seismic data. J. Petrol. Sci. Eng. 139, 219–239. DOI: https://doi.org/10.1016/j.petrol.2016.01.029.

Evensen, G., 1994. Sequential data assimilation with a nonlinear quasi-geostrophic model using Monte Carlo methods to forecast error statistics. J. Geophys. Res.: Oceans 99 (C5), 10143–10162. DOI: https://doi.org/10.1029/94JC00572.

Fahimuddin, A., Aanonsen, S.I., Skjervheim, J.A., 2010. Ensemble based 4D seismic history matching: Integration of different levels and types of seismic data. SPE EUROPEC/EAGE Annual Conference and Exhibition. Society of Petroleum Engineers. DOI: https://doi.org/10.2118/131453-MS.

Formentin, H.N., Almeida, F.L.R., Avansi, G.D., Maschio, C., Schiozer, D.J., Caiado, C., Vernon, I., Goldstein, M., 2019. Gaining more understanding about reservoir behavior through assimilation of breakthrough time and productivity deviation in the history matching process. J. Petrol. Sci. Eng. 173, 1080-1096. DOI: https://doi.org/10.1016/j.petrol.2018.10.045.

Fossum, K., Lorentzen, R.J., 2019. Assisted history matching of 4D seismic data - A comparative study. Petroleum Geostatistics vol. 2019. European Association of Geoscientists & Engineers, pp. 1–5, 1. DOI: https://doi.org/10.3997/2214-4609.201902180.

van Gestel, J.P., Best, K.D., Barkved, O.I., Kommedal, J.H., 2011. Integration of the life of field seismic data with the reservoir model at the Valhall field. Geophys. Prospect. 59, 673–681. DOI: https://doi.org/10.1111/j.1365-2478.2011.00946.x.

Leeuwenburgh, O., Arts, R., 2014. Distance parameterization for efficient seismic history matching with the ensemble Kalman filter. Comput. Geosci. 18, 535–548. DOI: https://doi.org/10.1007/s10596-014-9434-y.

Lorentzen, R.J., Bhakta, T., Grana, D., Luo, X., Valestrand, R., Nævdal, G., 2020. Simultaneous assimilation of production and seismic data: application to the Norne field. Comput. Geosci. 24, 907–920. DOI: https://doi.org/10.1007/s10596-019-09900-0.

Maleki, M., Davolio, A., Schiozer, D.J., 2017. Using simulation and production data to resolve ambiguity in interpreting 4D seismic inverted impedance in the Norne Field. Petroleum Geoscience, 24, 335–347. DOI: https://doi.org/10.1144/petgeo2017-032.

Maleki, M., Danaei, S., Silva, F.B.M., Davolio, A., Schiozer, D.J., 2021. Stepwise uncertainty reduction in time-lapse seismic interpretation using multi-attribute analysis. Petroleum Geoscience, 27. DOI: https://doi.org/10.1144/petgeo2020-087.

Maleki, M., Schiozer, D.J., Davolio, A. and Lopez, J., 2022. A Workflow for High-Resolution Reservoir Characterization using Multiple 4D Seismic Datasets. ECMOR Vol. 2022, No. 1, pp. 1-13. European Association of Geoscientists & Engineers. DOI: https://doi.org/10.3997/2214-4609.202244015.

Maschio, C., Schiozer, D.J., 2016. Probabilistic history matching using discrete Latin Hypercube sampling and nonparametric density estimation. J. Petrol. Sci. Eng. 147, 98–115. DOI: https://doi.org/10.1016/j.petrol.2016.05.011.

Maschio, C., Avansi, G.D., Silva, F.B.M., Schiozer, D.J., 2022. Data assimilation for uncertainty reduction using different fidelity numerical models. J. Petrol. Sci. Eng. 109851. DOI: https://doi.org/10.1016/j.petrol.2021.109851.

Neto, G.M.S., Davolio, A., Schiozer, D.J., 2021. Assimilating time-lapse seismic data in the presence of significant spatially correlated model errors. J. Petrol. Sci. Eng. 109127. DOI: https://doi.org/10.1016/j.petrol.2021.109127.

Oliver, D.S., Fossum, K., Bhakta, T., Sandø, I., Nævdal, G., Lorentzen, R.J., 2021. 4D seismic history matching. J. Petrol. Sci. Eng. 109119. DOI: https://doi.org/10.1016/j.petrol.2021.109119.

Paiaman, A.M., Santos, S.M.G., Schiozer, D.J., 2021. A review on closed-loop field development and management, J. Petrol. Sci. Eng. 108457. DOI: https://doi.org/10.1016/j.petrol.2021.108457.

Rosa, D.R., Schiozer, D.J., Davolio, A., 2022. Impact of model and data resolutions in 4D seismic data assimilation applied to an offshore reservoir in Brazil. J. Petrol. Sci. Eng. 110830. DOI: https://doi.org/10.1016/j.petrol.2022.110830.

Santos, J.M.C., Rosa, D.R., Schiozer, D.J., Davolio, A., 2022. Fast diagnosis of reservoir simulation models based on 4D seismic similarity indicators. J. Petrol. Sci. Eng. 110083. DOI: https://doi.org/10.1016/j.petrol.2021.110083.

Schiozer, D.J., Santos, A.A.S., Santos, S.M.G., Hohendorff Filho, J.C.V., 2019. Model based decision analysis applied to petroleum field development and management. Oil Gas Sci. Technol. 74, 1–20. DOI: https://doi.org/10.2516/ogst/2019019.

Silva, F.B.M., Davolio, A., Schiozer, D.J., 2015. A Systematic Approach to Uncertainty Reduction with a Probabilistic and Multi-Objective History Matching. Paper number: SPE-174359. SPE EUROPEC. DOI: https://doi.org/10.2118/174359-MS.

Silva Neto, G.M., Soares, R.V., Evensen, G., Davolio, A., Schiozer, D.J., 2021. Subspace ensemble randomized maximum likelihood with local analysis for time-lapse-seismic-data assimilation. SPE J. 26 (2), 1011–1031. DOI: https://doi.org/10.2118/205029-PA.

Soares, R.V., Maschio, C., Schiozer, D.J., 2018. Applying a localization technique to Kalman gain and assessing the influence on the variability of models in history matching. J. Petrol. Sci. Eng. 169, 110–125. DOI: https://doi.org/10.1016/j.petrol.2018.05.059.

Soares, R., Luo, X., Evensen, G., Bhakta, T., 2020. 4D seismic history matching: Assessing the use of a dictionary learning based sparse representation method. J. Petrol. Sci. Eng. 107763. DOI: https://doi.org/10.1016/j.petrol.2020.107763.

Yin, Z., Feng, T., MacBeth, C., 2019. Fast assimilation of frequently acquired 4D seismic data for reservoir history matching. Comput. Geosci. 128, 30–40. DOI: https://doi.org/10.1016/j.cageo.2019.04.001.

Silva, F. B. M.: Methodology, Formal analysis, Investigation, Writing - Original Draft, Writing - Review & Editing; **Davolio, A.:** Conceptualization, Writing - Review & Editing, Project administration; **Schiozer, D. J.:** Validation, Supervision, Resources.